Modeling the wind structure of AG Peg by fitting of C IV and N V resonance doublets

Eriksson, Mattias; Johansson, Sveneric; Wahlgren, Glenn

Published in:
Astronomy & Astrophysics

DOI:
10.1051/0004-6361:20034086

2004

A&A 422, 987–999 (2004)
DOI: 10.1051/0004-6361:20034086

Astronomy & Astrophysics

Modeling the wind structure of AG Peg by fitting of C IV and N V resonance doublets

M. Eriksson[1,2], S. Johansson[2], and G. M. Wahlgren[2]

[1] University College of Kalmar, 391 82 Kalmar, Sweden
[2] Lund Observatory, Lund University, Box 43, 22100 Lund, Sweden
e-mail: mattias@astro.lu.se

Received 16 July 2003 / Accepted 31 March 2004

Abstract. The latest outburst of AG Peg has lasted for 150 years, which makes it the slowest nova eruption ever recorded. During the time of *IUE* observations (1978−1995) line profiles and intensity ratios of the N V and C IV doublet components changed remarkably, and we discuss plausible reasons. One of them is radiative pumping of Fe II which is investigated by studying the fluorescence lines from pumped levels. Three Fe II channels are pumped by C IV and one by N V. The pumping rates of those Fe II channels as derived by the modeling agree well with the strengths of the Fe II fluorescence lines seen in the spectra. We model the C IV and N V resonance doublets in *IUE* spectra recorded between 1978 and 1995 in order to derive optical depths, expansion velocities, and the emissivities of the red giant wind, the white dwarf wind and their collision region. The derived expansion velocities are ∼60 km s^{-1} for the red giant wind and ∼700 km s^{-1} for the white dwarf wind. We also suggest a fast outflow from the system at ∼150 km s^{-1}. The expansion velocity is slightly higher for N V than for C IV. Emission from the collision region strongly affects the profile of the N V and C IV resonance doublets indicating its existence.

Key words. atomic processes – line: formation – line: profiles – stars: binaries: symbiotic – stars: individual: AG Peg

1. Introduction

The symbiotic stars are a subclass of interacting binaries consisting of a red giant and a hot radiation source, both of solar-like mass. The two stars are embedded in an ionized common envelope formed by the stellar winds of the stars and sometimes also material ejected during outburst. A common phenomenon in symbiotic stars is the accretion of material from the red giant onto the white dwarf, which can lead to nova-like eruptions (Tomov & Tamova 2001). In the ultraviolet region the spectrum of symbiotic stars is dominated by emission lines from different sources. The nebular emission lines have three different possible origins: the thick inhomogeneous wind from the red giant, the fast wind from the white dwarf, and/or from a region where the two winds collide (Mürset et al. 1997; Vogel & Nussbaumer 1994). A fraction of the wind from the red giant is photoionized by the UV emission from the hot component, which explains the observed nebular emission lines from higher ionization stages such as C^{3+}, N^{4+}, O^{3+}, Si^{3+}, and S^{2+}. A complication in the interpretation of the UV spectrum of symbiotic stars is that the Fe^{+} ions in the common envelope fluoresce when irradiated by the strong UV emission lines (Johansson 1983).

The star AG Peg (BD+11°4673) underwent a nova eruption sometime between 1841 and 1855 (Lundmark 1921). The luminosity increased from about 9th to a maximum of about 6th mag around 1885. During the first 70 years after detection of the nova eruption the spectrum of AG Peg slowly evolved from a P Cygni type (H I, He II emission lines showed P Cygni profiles) to a combined spectrum originating from a hot component, a nebular region and a M 3 red giant (Merrill 1951). AG Peg is also classified as a symbiotic nova (Allen 1980), and it is believed to be the slowest nova ever observed, as the bolometric luminosity was nearly constant until the late 1970s when it started to decline.

There has been an ongoing discussion about the wind structure in symbiotic systems in general (Girard & Willson 1987) and in AG Peg in particular (Vogel & Nussbaumer 1994, 1995). This is of great interest since some symbiotic systems could be progenitors of type Ia supernovae (Munari 1994; Boffi et al. 1994). It is of basic importance to model the wind structure for our understanding of the observed line profiles and spectral variability in symbiotic systems. The strong nebular emission lines in the spectrum of AG Peg have changed significantly between 1978 and 1995. This gives an excellent opportunity to derive parameters such as wind velocities, temperatures and opacities in different regions of the symbiotic nebula.

In the present work we have fitted theoretical line profiles to the C IV and N V resonance doublets observed in *IUE* spectra to derive both the wind structure and evolution of the nebula during the time 1978−1995. The starting values of the parameters used in the theoretical spectra, such as wind velocities,

Table 1. *IUE* spectra used in this work.

Spectrum	Exp. (s)	Aperture*	Obs. date	Spectrum	Exp. (s)	Aperture*	Obs. date
SWP02326	1200	L	18 Aug. 1978	SWP40148	900	L	20 Nov. 1990
SWP02334	6000	L	18 Aug. 1978	SWP40149	9000	L	20 Nov. 1990
SWP02953	2400	S	13 Oct. 1978	SWP43006	720	L	4 Nov. 1991
SWP05669	1800	S	29 Jun. 1979	SWP43007	13 980	L	4 Nov. 1991
SWP06353	1800	S	2 Sep. 1979	SWP46060	2700	L	5 Oct. 1992
SWP06355	4200	S	2 Sep. 1979	SWP46142	900	L	6 Nov. 1992
SWP06527	3960	L	15 Sep. 1979	SWP47697	720	L	20 May 1993
SWP06809	900	L	9 Oct. 1979	SWP50707	720	L	7 May 1994
SWP07406	1800	S	14 Dec. 1979	SWP52387	3600	L	12 Oct. 1994
SWP08760	1800	S	14 Apr. 1980	SWP55055	900	L	21 Jun. 1995
SWP09807	1440	L	23 May 1980	LWR02591	1200	S	13 Oct. 1978
SWP10454	1440	L	23 Oct. 1980	LWR06389	3600	S	14 Dec. 1979
SWP11004	900	L	9 Jan. 1981	LWR09130	2700	L	23 Oct. 1980
SWP13975	900	L	10 May 1981	LWR10571	840	L	10 May 1981
SWP15649	840	L	4 Dec. 1981	LWP09698	3000	L	12 Dec. 1986
SWP15651	6600	L	4 Dec. 1981	LWP16684	1800	L	28 Oct. 1989
SWP29862	10 800	L	12 Dec. 1986	LWP19253	1200	L	20 Nov. 1990
SWP29863	1500	L	13 Dec. 1986	LWP21635	1200	L	4 Nov. 1991
SWP37046	1800	L	16 Sep. 1989	LWP24280	1800	L	6 Nov. 1992
SWP37420	600	L	21 Oct. 1989	LWP25995	3600	L	25 Jul. 1993
SWP37476	1800	L	28 Oct. 1989	LWP28122	3900	L	13 May 1994
SWP37477	11 160	L	28 Oct. 1989	LWP30936	1080	L	21 Jun. 1995

* L = Large aperture; S = Small aperture.

optical depths and fluxes, are based upon previous work on AG Peg as well as assumptions made in this work. These parameters were varied in narrow ranges that satisfy our assumptions in order to get better agreement between observed and theoretical spectra. It is also our intent to understand to what extent the pumping of Fe II affects the line profiles and intensity ratios of the C IV and N V fine structure components. We have studied the flux in the Fe II fluorescence lines generated by the C IV and N V doublets. Selective pumping of Fe II was incorporated in the theoretical spectra and the possible ranges for the wavelengths and optical depths of the pumping channels were set by analysing the corresponding fluorescence lines. As a result of fitting many *IUE* spectra we were able to detect changes in the system and determine some parameters to good accuracy.

2. Data

Many high-dispersion spectra of AG Peg were recorded by the *IUE* satellite during its lifetime (1978−1995). These data were extracted from the Multimission Archive at Space Telescope (MAST) and provide heliocentric wavelengths and flux calibrated intensities. Due to the relative close proximity of AG Peg (1.3 kpc) no correction for interstellar extinction was made to the intensity data. Uncertainties in the absolute flux value are of limited importance for the fitting of the C IV and N V resonance doublets (see below) since only the relative intensities of the components are modeled. Each of these doublets is entirely within a single echelle order, thereby alleviating the need to consider order-to-order variations in wavelength and flux when discussing the doublet structure.

The spectra used in this study are listed in Table 1. Images from the Short Wavelength Prime (SWP) camera provided the line profiles for the C IV and N V doublets and a few pumped channels of Fe II. The bulk of the Fe II fluorescence lines are located at the wavelengths of the Long Wavelength Redundant (LWR) and Long Wavelength Prime (LWP) cameras. The long wavelength spectra chosen for analysis occur at epochs as close as possible to the SWP spectra. Unfortunately, there are large gaps in the temporal coverage of the data, with no observations of AG Peg having been taken from January 1982 until September 1989, with the exception of December 1986. The available spectra had been obtained for a range of exposure times and some of them are affected by saturation for strong lines, including the C IV and N V doublets.

3. The N V and C IV resonance doublets

The isoelectronic ions C^{3+} and N^{4+} have the same atomic structure, and the resonance doublet in C IV and N V corresponds to the transition 2s ^{2}S−2p ^{2}P. The resonance lines in C IV appear at 1548.2 Å (J = 1/2−J = 3/2) and 1550.8 Å (1/2−1/2) and in N V at 1238.8 Å (1/2−3/2) and 1242.8 Å (1/2−1/2). The intensity ratio in the doublet is expected to follow the statistical weights, i.e. I(1/2−3/2)/I(1/2−1/2) = 2, which is verified by theoretical calculations of the Einstein A-values (Warner 1968). Besides the strictly parity-forbidden lines of

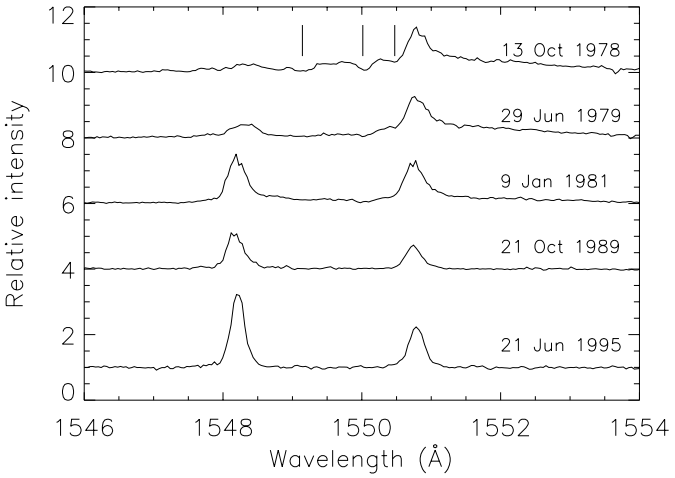

Fig. 1. The temporal development of the C IV resonant doublet. The data from 1986 are not incorporated in the figure since the doublet was saturated. The three absorption features in early *IUE* spectra discussed in the text are marked in the figure. The spectra have been shifted in relative intensity for plotting purposes and the intensity of the two uppermost spectra in the figure are multiplied by a factor of two.

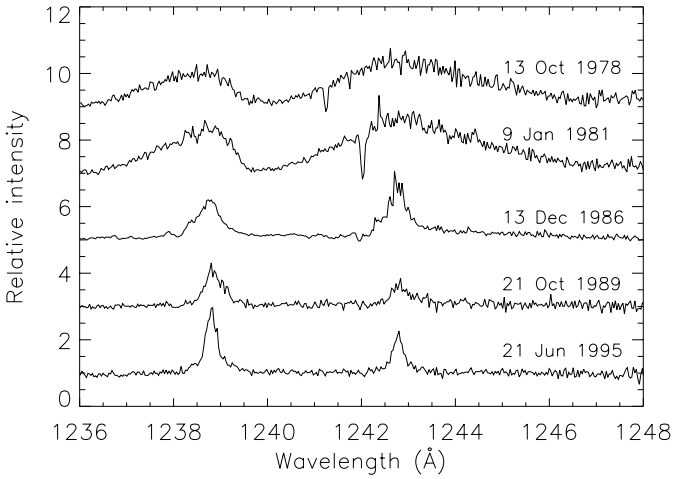

Fig. 2. The temporal development of the N V resonant doublet. The intensity of the spectrum recorded on 13 Oct. 1978 is multiplied by a factor of 4 and the spectrum from 9 Jan. 1981 is multiplied by 2. The sharp, deep absorption features in the two uppermost spectra are data artefacts.

multiply-charged ions the C IV and N V resonance doublets are important temperature indicators and can be used for diagnostics of the dynamics of energetic stellar winds. They have therefore been a popular target in satellite UV observations, in particular with *IUE*. The lines often show a complicated multi-component structure.

The composite structure of the C IV and N V resonance lines has changed noticeably during the period 1978−1995 as shown in Figs. 1 and 2. The multi-component structure has been discussed by Kenyon et al. (1993), who suggested emission contributions from at least two different regions, the white-dwarf wind and the red-giant upper atmosphere. The white-dwarf wind has a terminal velocity of 900 km s^{-1} (Penston & Allen 1985), emitting the broad C IV and N V components with widths of 500 km s^{-1}. It is believed to be denser than the surrounding nebula, leading to observed P Cygni profiles. The red-giant atmosphere, which is heated by the UV radiation from the white dwarf, shows the narrow component with Gaussian widths of about 70 km s^{-1}. A third emission component, originating from the region where the winds of the red giant and the white dwarf collide, was introduced by Nussbaumer et al. (1995), who also clearly demonstrated the presence of a broad and a narrow component.

In our model we have included four regions in AG Peg contributing to the composite line structure of the C IV and N V resonance lines. Line emission results from the white-dwarf wind, from two separate velocity components in the red-giant wind and from the collision region. The total line profile is also affected by blueshifted absorption from the wind regions as well as the surrounding nebula, producing P Cygni profiles.

The expected intensity ratio of the two fine-structure lines in C IV and N V is 2, but in several symbiotic systems this ratio has been observed by Michalitsianos et al. (1992) to be noticeably less than 2, sometimes even below 1. They studied the possible effect on the profile of the C IV λ1548.2 line from resonant photoexcitation of Fe II by C IV photons, as observed in *IUE* spectra of RR Tel (Johansson 1983). However, they could not explain the intensity anomaly based on this Bowen-type process. The *IUE* spectra illustrate that intensity anomalies are clearly present in AG Peg, especially during the years 1978−1981 when the intensity ratio is less than 1 (Fig. 1). In Sect. 4 we discuss in detail all Fe II pumping processes observed in AG Peg involving the C IV and N V resonance lines.

A recent explanation for the strange intensity ratio of the C IV and N V lines observed in symbiotic stars has been presented by Yoo et al. (2002). They proposed that, if bipolar winds are present in the system, double scattering can occur, where intensity is transferred from the blue line to the red line due to an internal Doppler effect. The process requires an acceleration that produces a bipolar wind velocity exceeding the fine-structure interval of the doublets, which corresponds to 500 km s^{-1} for C IV and 970 km s^{-1} for N V. The double scattering process has not been considered in this work, which we comment on in Sect. 5.

We describe below in detail the time history of the C IV and N V line profiles. The two fine-structure components of each spectrum are called the blue and the red line, respectively, based on their relative wavelengths. The different emission and absorption contributions in each line will be called components, e.g. WD (white dwarf) component and RG (red giant) component.

3.1. The C IV resonance doublet in AG Peg

The time history of the C IV resonance doublet in AG Peg is illustrated in Fig. 1 by the *IUE* spectra. In the first spectrum of 1978 it had a rather complex appearance: the blue line was nearly absent while the red line was one of the strongest in the entire ultraviolet spectrum. It is easily discerned that the lines originated from at least two different spatial regions of AG Peg, since the red line consists of a base with the Gaussian width

of 2.6 Å and a nebular component of width 0.2 Å. The broad WD component had a similar peak intensity as the narrow RG component (as determined from the modeling in Sect. 5).

Three absorption features (marked by vertical lines in Fig. 1) are observed in the blue wing of the red line. The one closest to the emission peak is weak and is the P Cygni absorption component of the RG narrow line, since it is of equal width (0.2 Å) and shifted only by ~ -50 km s^{-1} from the emission component. The second absorption line is shifted by ~ -170 km s^{-1} and broader than the RG component. It could be due to a fast outflow from the red giant as suggested for the symbiotic binary V2116 Oph (Chakrabarty et al. 1998). The third absorption line is broader (1.2 Å) and has a velocity shift of ~ -340 km s^{-1}, corresponding most likely to the collision region, i.e. where the winds of the two stars collide (Nussbaumer et al. 1995).

During 1978–1981 the C IV profiles change notably. The intensity of the WD component decreases relative to the RG component so that less than ~5% of the red C IV feature consists of the broad base component in December 1981. The shrinking WD component seems to be accompanied by reduced absorption from the white dwarf wind. The blue C IV line strengthened continuously relative to the red line and by January 1981 the intensity ratio reached 1. There were no *IUE* observations of AG Peg from 1982 until the end of 1986.

In the 1986 spectra the WD component is barely detectable, and there are no visible absorption lines associated with the RG wind, the collision region or the surrounding nebula. However, based on the modeling in Sect. 6 they still contribute to the observed features. The C IV intensity ratio seems to have continued to increase but no reliable value can be obtained since the lines are saturated in both spectra recorded in 1986. After 1986 there are another two years without *IUE* observations of AG Peg.

In the spectrum of 1989 the lines of the C IV doublet are much narrower than in 1986. This implies that the trend of growing emission from the collision region probably has ended and that the emission from the RG atmosphere is now dominating. During the years between 1989 and 1995 the intensity ratio continued to rise, from ~1.5 in 1989 to ~1.8 in 1995, probably because of decreasing opacity in the WD wind. The C IV emission from the WD wind disappeared from the *IUE* spectra having the longest exposure time during the early 1990s, but was observed in spectra recorded with the *HST* GHRS instrument, which has a higher sensitivity (Nussbaumer et al. 1995).

3.2. The N V resonance doublet in AG Peg

In 1978 the N V resonance doublet appeared in the *IUE* spectrum as two broad features originating from the WD wind (Fig. 2). No narrow RG components were detectable. The N V lines had also an anomalous intensity ratio, ~0.7, but not to the same extent as C IV, for which the blue line was barely noticeable. If the terminal velocity of the WD wind is close to 900 km s^{-1}, as suggested by Penston & Allen (1985), the absorption of the red line (λ1242.78) is blue-shifted by 3.8 Å and will fall just to the red of the blue N V line (λ1238.80). One would therefore expect a higher intensity ratio for the N V doublet than for the C IV ratio in 1978. The blue line is narrower than the red line. The line profile fitting in Sect. 5 implies that, because of geometrical properties of the symbiotic system, the emission from the wind collision region is not absorbed to the same extent as the white dwarf wind emission.

During the next three years, through May 1981, there was no significant change in the N V doublet. The intensity ratio slowly increased to ~0.9, and a weak absorption feature blue-shifted by ~ -250 km s^{-1} is seemingly present in some of the spectra. However, by December 1981 remarkable differences are observed. The blue wing of the red N V line becomes totally absorbed while the blue line appears narrower with a *FWHM* of ~0.9 Å. The peak intensity ratio continued to increase and reached 1.0 in 1981.

By 1986 the broad WD component nearly vanished while strong emission in the RG component dominated the spectrum. As for the C IV doublet, at this time both lines stood on a socket that most likely originated from the collision region. Surprisingly, the peak intensity ratio (~0.6) has decreased again and is nearly back to the 1978 value. Except for the WD absorption three other absorption features, each of them associated with N V, are observed in long exposure spectra during 1986. They have blue-shifts of -190, -340 and -470 km s^{-1}, and the first two correspond to similar absorption features seen at an earlier stage in C IV. These two are associated with the fast RG component and the collision region, respectively.

In 1989 the intensity ratio has increased to 1.2, and the two lines have become more narrow (*FWHM* of ~0.5 Å). This was also observed for C IV. Hence, the N V radiation is now dominated by the RG region facing the white dwarf. Both lines still rest on a socket, which has decreased in strength since 1986. The only absorption line clearly remaining is the feature corresponding to the surrounding nebula. During 1989–1995 the intensity ratio continued to rise until it reached the value of 2 in 1995. In the early 1990s a narrow absorption feature appeared slightly red-shifted relative to the narrow nebular component of the red λ1242.78 line. It will be shown in Sect. 4 that it is due to resonant pumping of Fe II. The WD wind is not observed in N V in *IUE* spectra after 1989, but it has been observed with the more sensitive *HST*/GHRS instrument (Nussbaumer et al. 1995) where a continuing decline of the N V emission from the white dwarf wind was detected. Although no C IV or N V emission from the WD wind is observed in *IUE* spectra after 1989, Altamore & Cassatella (1997) showed that WD wind emission is still detectable after 1989 in the He II λ1640 and N IV] λ1487 lines.

4. N V and C IV pumped Fe II lines

4.1. The fluorescence processes

Based on early *IUE* spectra of RR Tel (Penston et al. 1983) several strong lines were identified by Johansson (1983) as fluorescence lines of Fe II, excited by C IV in a Bowen mechanism. The possible connection between a part of the blue C IV line intensity being transferred to Fe II and the anomalous intensity ratio of the C IV doublet observed in

Table 2. Observed and corrected intensity ratios of the C IV doublet, $I(1548.2)/I(1550.8)$.

Star	Observed[a]	Corrected[b]
Z And	1.54	2.00
EG And	1.41	1.48
V 1016 Cyg	1.31	1.67
RW Hya	1.66	1.70
SY Mus	1.28	1.36
AG Peg	0.77	1.01
RX Pup	0.57	0.81
RR Tel	1.16	1.62

[a] Measured from *IUE* spectra.
[b] After adding the flux deficit caused by fluorescence.

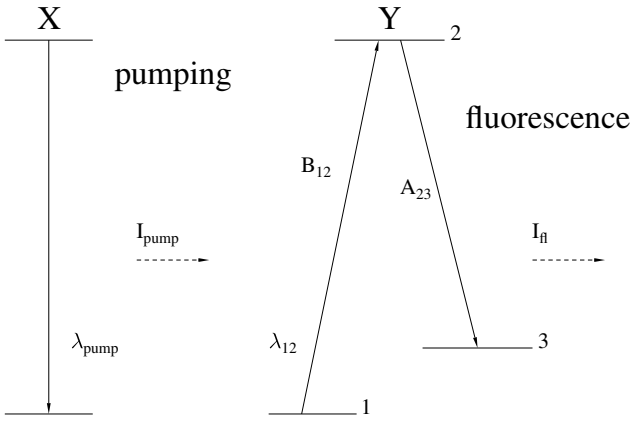

Fig. 3. Scheme showing photoexcitation by an accidental resonance, i.e. $\lambda_{\rm pump} \sim \lambda_{12}$. A strong line from spectrum X pumps the $1 \rightarrow 2$ transition in Y, which results in the fluorescence line $2 \rightarrow 3$ with intensity $I_{\rm fl}$. B_{12} and A_{23} are Einstein coefficients.

symbiotic systems was investigated by Michalitsianos et al. (1992). An influence of Fe II pumping seemed likely since Johansson (1983) had found 10 strong UV lines of Fe II, originating from one particular Fe II level, $y^4H_{11/2}$ in RR Tel spectra. This level is pumped by C IV through the excitation channel $a^4F_{9/2}$–$y^4H_{11/2}$ at 1548.204 Å, coinciding with the blue C IV line at 1548.187 Å. To estimate the optimal relative influence of the C IV pumping we have in Table 2 corrected the observed intensity ratio of the C IV doublet by adding the energy loss in the λ1548 line for eight symbiotic systems (Eriksson et al. 2001). The energy loss is obtained by adding the radiation energy in all of the observed Fe II fluorescence lines. The variation in the relative influence among the stellar systems may be due to inclination of the orbital plane. One of the purposes of the present work is to include the Fe II absorption in the modeling of the C IV and N V doublets in AG Peg, derive the line opacities for the pumped channels, and compare the derived and observed strength of the Fe II fluorescence lines. Another Fe II line has been identified in this work as a fluorescence line pumped by N V, and the Fe II line opacity has therefore been incorporated in the fitting of the N V doublet.

4.2. The Fe II fluorescence lines

Fluorescence processes based on photoexcitation by accidental resonances (PAR) require specific circumstances. Since the lower level in the pumped channel must have a significant population, the selective excitation mostly occurs from levels with low excitation energies. In thermal equilibrium photoexcitation from most metastable levels of Fe II requires temperatures of several thousand Kelvin to be detectable. The nebular temperature of AG Peg is estimated to be higher than 10 000 K (Michalitsianos et al. 1992). Radiative pumping in Fe II from the $b^2P_{3/2}$ level at an energy as high as 3.20 eV has been observed in RR Tel (Hartman & Johansson 2000), which is a symbiotic system with a spectrum similar to AG Peg. The possibility of selective photo excitation from levels up to 4 eV has been considered in this investigation. The pumping efficiency declines exponentially with an increasing wavelength difference between the center of gravity of the pumping line and the fluorescence channel. Therefore, resonant photoexcitation for separations greater than the *FWHM* of the pumping line is not likely to occur.

The intensity of a fluorescence line, $I_{\rm fl}$, in spectrum "Y" (in this case Y = Fe II) pumped by an emission line from an ion "*X*" (in this work *X* = C IV or N V) is given by

$$I_{\rm fl} \propto I_{0X} \cdot N_1 \cdot B_{12} \cdot A_{23} \cdot {\rm e}^{\frac{-(\lambda_X - \lambda_{\rm Fe})^2}{w^2}}, \quad (1)$$

where w is the Gaussian width of the pumping line, A and B are the Einstein coefficients for spontaneous decay and stimulated absorption, I_{0X} is the peak intensity of the pumping line and N_1 is the population of level 1 (Fig. 3). The two previously known Fe II channels, resonantly pumped by C IV λ1548.19, are $a^4F_{9/2}$–$y^4H_{11/2}$ at 1548.20 Å and $a^4P_{1/2}$–$w^2D_{3/2}$ at 1548.41 Å, and they coincide in wavelength with the strong C IV RG emission. Eighteen Fe II fluorescence lines originating from these two channels have been identified in *IUE* spectra of AG Peg (Eriksson et al. 2001). One new Fe II channel, $a^4\ F_{7/2}$–$y^2D_{5/2}$ at 1548.70 Å, also pumped by the blue C IV line, is added in the present work. A total of 26 C IV pumped fluorescence lines of Fe II are observed in AG Peg and reported in Table 3. The new fluorescence channel is of particular interest since it is too far in wavelength from the center of the C IV line to be pumped by the narrow, strong RG component and must be pumped by the wide component from the white dwarf wind.

The N V resonance doublet is also responsible for photoexcitation of Fe II. The emission line at 2605.82 Å (see Table 3) is a transition from $v^2G_{7/2}$ having an excitation energy of 10.33 eV, which is too high to be collisionally populated. However, the channel $a^4F_{5/2}$–$v^2G_{7/2}$ at 1242.74 Å coincides with the RG component of the N V λ1242.80 line resulting in selective population of $v^2G_{7/2}$ in Fe II. The λ2605.82 line is the only line observed from $v^2G_{7/2}$, since its branching fraction is more than three times higher than for any other transition from the same upper level (Fuhr et al. 1988). Since λ2605 is only slightly above the noise level, other transitions from $v^2G_{7/2}$ are too weak to be detected.

Of the seven strongest fluorescence lines in Table 3 six fall in the wavelength region 2435–2595 Å. These lines, in particular λ2493.1, are actually among the most prominent lines in

Table 3. Fe II fluorescence lines observed in AG Peg.

Pumping	Pumped level	Lower level	$\lambda_{\rm lab}$ (Å)[a]	Peak intensity[b]
Pumping line:				
Narrow C IV λ1548.187	$y^4H_{11/2}$	$a^2G_{9/2}$	1975.55	5
Pumped channel:		$a^2H_{11/2}$	2168.11	3
1548.204 Å		$a^4H_{13/2}$	2211.81	3
		$a^4H_{11/2}$	2220.59	12
		$a^4H_{9/2}$	2228.07	12
		$b^4F_{9/2}$	2281.73	2
		$a^4G_{11/2}$	2436.96	28
		$a^4G_{9/2}$	2459.53	27
		$b^2H_{11/2}$	2481.80	36
		$b^2H_{9/2}$	2493.10	44
		$b^2G_{9/2}$	2772.00	32
		$a^2I_{13/2}$	2977.26	1
		$c^2G_{9/2}$	3030.57	1
Pumped channel:	$w^2D_{3/2}$	$a^2F_{5/2}$	1965.92	1
1548.411 Å		$b^2F_{5/2}$	2142.46	6
		$c^2D_{5/2}$	2479.98	33
		$c^2D_{3/2}$	2483.08	27
		$c^2F_{5/2}$	2979.95	8
Pumping line:	$v^2G_{7/2}$	$c^2F_{5/2}$	2605.82	3
Narrow N V λ1242.804				
Pumped channel:				
1242.741 Å				
Pumping line:				
Broad C IV λ1548.187	$y^2D_{5/2}$	$a^4F_{5/2}$	1558.54	5
Pumped channel:		$b^2P_{3/2}$	2426.42	2
1548.697 Å		$a^4G_{7/2}$	2437.90	1
		$a^2F_{7/2}$	2519.81	3
		$a^2F_{5/2}$	2539.35	1
		$b^4D_{3/2}$	2806.15	1
		$b^4D_{5/2}$	2808.00	2

[a] Vacuum wavelengths.
[b] Mean value of the peak intensities during 1978−1995 in units of 10^{-13} erg cm^{-2} s^{-1} Å^{-1}.

the entire *IUE* spectrum of AG Peg recorded in the long wavelength region (2000−3300 Å). Four of these lines are displayed in Fig. 4.

4.3. Evolution of Fe II fluorescence lines during 1978 to 1995

As discussed in the previous section the C IV and N V doublets, which generate many Fe II fluorescence lines, have variable intensity and structure in the spectra of AG Peg during the years of *IUE* data collection. Variability is also observed in the fluorescence lines given in Table 3. Two of the C IV pumped channels coincide with the RG component of the blue C IV line (1548.187 Å), whereas the third one, at 1548.697 Å, is outside the width of this component. The time history of the corresponding fluorescence lines should therefore correlate differently with the time history of the composite structure of the C IV line. In Fig. 5 we show the time history of the Fe II fluorescence produced by pumping by the blue C IV line from the RG and WD components.

In the earliest *IUE* spectra of AG Peg, recorded before 1980, the blue C IV line is almost absent because of overlapping absorption from the P Cygni profile of the red C IV line. Nevertheless, the fluorescence lines pumped by the blue line are present in the same *IUE* spectra. This could imply that the pumping of iron occurs in a region located closer to the symbiotic system than the region responsible for the P Cyg absorption part of the WD component. However, the detailed modeling in Sect. 5 shows that the fluorescence takes place in the outermost part of the system. In any case, the red line

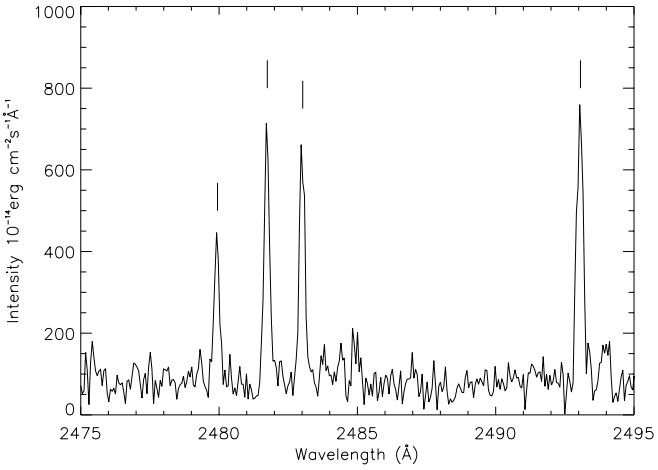

Fig. 4. C IV pumped Fe II fluorescence lines $\lambda\lambda$2479.98, 2481.80, 2483.08, 2493.10, in AG Peg identified in the *IUE* spectrum LWP25995 (recorded 25 July 1993).

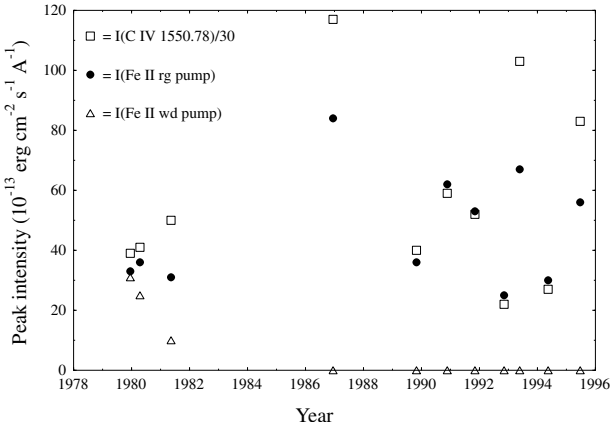

Fig. 5. Temporal behaviour of C IV λ1550.78 and the C IV pumped fluorescence of Fe II. The filled circles correspond to the intensity of the Fe II λ2493.10 line pumped by the red giant emission and the triangles correspond to the sum of the intensity of the observed Fe II lines produced by pumping of the white dwarf.

seems to best represent the flux in C IV. Therefore, we have plotted in Fig. 6 the correlation between the peak intensity of the red line (and not the true pumping line, the blue line) with the peak intensities of two Fe II fluorescence lines. We used one Fe II line from each of the levels 4p $y^4H_{11/2}$ (λ2493.10) and 4p $w^2D_{3/2}$ (λ2479.98), and the C IV and Fe II intensities were measured in the LWP and SWP spectra recorded close in time to each other. Figure 6 shows that there is a good intensity correlation between the fluorescence lines and the red C IV line. This indicates that the first two groups of Fe II lines listed in Table 3 are generated by C IV. It may also indicate that the problem with the varying C IV intensity ratio is due to the blue line and a combination of absorption due to the red line P Cyg profile and to fluorescent pumping. This will further be discussed in Sect. 5.

We have applied a linear least squares fitting to the data in Fig. 6 and found the following correlations between the peak

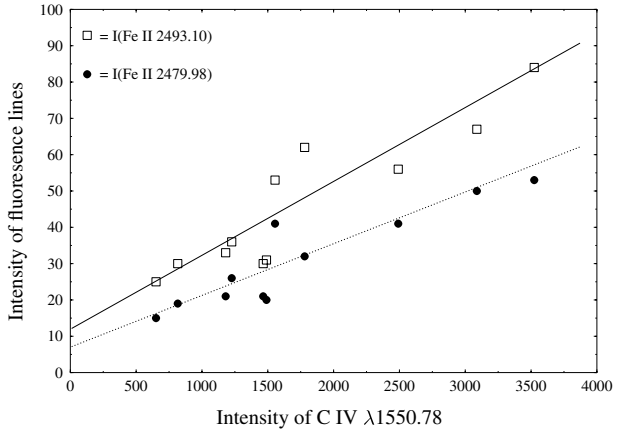

Fig. 6. Correlation between Fe II fluorescence lines and C IV λ1550.78. Intensites are given in units of 10^{-13} erg cm^{-2} s^{-1} Å^{-1}.

intensity of the Fe II fluorescence lines and the peak intensity of C IV:

$$I(\lambda 2493.10) = 0.0193 \cdot I(\lambda 1550.77) + 12.301 \times 10^{-13}, \quad (2)$$

$1\sigma = 4.9 \times 10^{-13}$, and

$$I(\lambda 2479.98) = 0.0135 \cdot I(\lambda 1550.77) + 7.176 \times 10^{-13}, \quad (3)$$

$1\sigma = 3.8 \times 10^{-13}$,

where the intensities are in units of erg cm^{-2} s^{-1} Å^{-1}. By using Eqs. (2) and (3), respectively, we can express the optical depth, τ, at the wavelengths corresponding to the pumping channels $a^4F_{9/2}$–$y^4H_{11/2}$ (1548.20 Å) and $a^4P_{1/2}$–$w^2D_{3/2}$ (1548.41 Å) in terms of the branching fraction, BF, by the following equation

$$e^{-\tau} = 1 - 0.5 \cdot \frac{dI_{fl}}{dI(1550.78)} \cdot \frac{\lambda_{fl}}{BF_{fl} \cdot 1548.187} \times \exp\left(\frac{\left(1548.187 - \lambda_p\right)^2}{w_p^2}\right), \quad (4)$$

where subscript "fl" refers to the fluorescence line and "p" to the pumped Fe II channel. The term $\frac{dI_{fl}}{dI(1550.78)}$ is the derivative of the intensity of the fluorescence line with respect to the pumping line and w_p is the Gaussian width of the pumping line. The branching fractions for the Fe II λ2493.10 and λ2479.98 lines are 0.045 and 0.36, respectively. This implies optical depths in the Fe II region of 0.43 at 1548.20 Å related to the pumping channel $a^4F_{9/2}$–$y^4H_{11/2}$ and 0.49 at 1548.41 Å related to the pumping channel $a^4P_{1/2}$–$w^2D_{3/2}$. The optical depths at the pumping channels $\lambda\lambda$2493, 2480 are restricted to be between 0.3–0.6 in the modeling in Sect. 5 in order to decrease the freedom of other parameters.

The third group of C IV pumped Fe II fluorescence lines in Table 3 is due to the pumping channel $a^4F_{7/2}$–$y^2D_{5/2}$ at 1548.70 Å, which is outside the reach of the RG component in the blue C IV line. The fluorescence lines are clearly present in *IUE* spectra of AG Peg during 1978–1981. When, after five years without observations (Fig. 4), AG Peg was observed again during 1986–1995 there were no traces of these lines.

This is in agreement with the disappearance of the C IV lines after 1986, as discussed in Sect. 3.2.

The λ2605.82 line in Table 3 is the only observed Fe II line associated with the pumping channel $a^4F_{5/2}-v^2G_{7/2}$ at 1242.74 Å, which is activated by the red N V line. This line is absent in the *IUE* spectra until 1993, when it became clearly observable, and remained so during the last two years of the *IUE* epoch.

5. Modeling the spectra and resulting parameter values

In the modeling we have treated the spectral regions of the C IV and N V doublets in AG Peg separately. In each of the two regions we have only included the two resonance lines and the Fe II lines pumped by them. The influence of potential minor contributors is unknown. The equations for the theoretical line profiles $F^X(\lambda)$ (X = C(arbon) or N(itrogen)) used to fit the observed C IV and N V resonance lines are constructed as follows (the indication that all functions involved are λ-dependent is excluded below):

$$F^X = A^X + \sum_j f_j^X, \tag{5}$$

where the first term A^X refers to the line profile obtained in the wind regions, and the second term refers to the effect of the fluorescent pumping in the outer nebular region. The term A^X consists of two parts

$$A^X = \sum_{i=1}^{5} d_i^X + \sum_{i=1}^{4} a_i^X, \tag{6}$$

where the first sum represents the emitted energy in the lines and the second sum the energy absorbed in intervening regions. The indices refer to five different sources and regions: the white dwarf (WD) wind, the slow component of the red giant (RG) wind, fast component of the RG wind, wind collision (WC) region, and the observed continuum level. The free parameters are the relative velocities between the different regions (some of them within certain limits) within the system and the optical depths of pumping and pumped transitions in C IV, N V and Fe II.

The main differences between this model and previous analyses (Vogel & Nussbaumer 1994; Nussbaumer et al. 1995) concern the absorption in the WD wind. We obtained the best fits assuming that the absorption of C IV and N V occurs at some distance from the white dwarf where the temperatures are sufficient for the respective ion, which leads to constant expansion velocity for each ion. We have also for the first time included pumping of Fe II in a fitting procedure of the resonance doublets.

Equation (5) is based on some assumptions about the symbiotic system AG Peg. Firstly, due to the slow nova eruption beginning in 1850 the white dwarf has a wind at a terminal velocity of ~1000 km s^{-1} according to Kenyon et al. (1993). The WD wind velocity is now treated as a free parameter (with certain limits) in the broad C IV and N V components. The WD wind is probably very extended and encloses most of the stellar system. The red giant looses also material in a dense, slow wind, for which we assume an expansion velocity typical of red giants (30 to 100 km s^{-1}). The radiative temperature varies with distance from the white dwarf and determines the ionization balance in the various regions. For example, matter in the RG extended atmosphere and wind becomes ionized by the WD UV emission. As the white dwarf evolves along the post-AGB phase its wind becomes more transparent for radiation, which leads to an increase in the radiative temperature. The ionization increases in the WD wind as well as in the RG region, which also starts to emit C IV and N V radiation.

Between the two stars there is a region where the dense RG wind collides with the fast WD wind heating the material mechanically to several million degrees Kelvin (Murset et al. 1995). We assume that the matter in the WC region has an expansion velocity close to half of the WD wind velocity since the particles in the WD wind loose momentum when colliding with the slower particles in the RG wind. We also assume that further out in a nebula surrounding the symbiotic system Fe^+ ions are pumped by emission lines originating from highly-ionized elements located in the WD wind, closer to the white dwarf.

These qualitative assumptions are expressed by quantitative expressions (see Appendix A) and included in Eqs. (5) and (6). The parameters have been changed iteratively to get an agreement between the theoretical and observed spectrum around the C IV and N V lines. Most of the parameters make independent effects on the spectrum. As starting values for some parameters, e.g. velocities, we have used previously published data, and for others, e.g. line width, we have extracted the values from similar lines. Assumptions the parameters presented in Appendix A were inserted into the equations, which were fitted to the observed line profiles. In Fig. 7 we show the result of our fit applying Eq. (5) to the C IV and N V resonance regions in AG Peg. In the following subsections we discuss both the resulting parameter values obtained from the fitting procedure and the development of the parameters studied in the various regions.

5.1. The white dwarf wind

For the years 1978−1981, the average WD wind velocity obtained from the fitting procedure is 650 ± 20 km s^{-1} for C IV and 700 ± 35 km s^{-1} for N V. According to the diagram in Fig. 8 it is then nearly constant for the whole *IUE* period 1978−1995, in agreement with the results of Altamore & Cassatella (1997). This means that the velocity is larger than the fine-structure splitting in C IV but not in N V.

Both the emission and the blue-shifted absorption of the C IV and N V lines in the WD wind weaken during the period of *IUE* observations as shown in Figs. 9 and 10. During Aug. 1978−Sep. 1979 the emitted intensity of the red C IV line in the WD wind is (7.9 ± 3.8) × 10^{-11} (erg cm^{-2} Å^{-1} s^{-1}, hereafter we use this intensity unit and denote it as i.u.), and the optical depth at the central wavelength of the blue-shifted C IV absorption is 1.66 ± 0.24. During the following two years (to Dec. 1981) the intensity of the wind component drops by

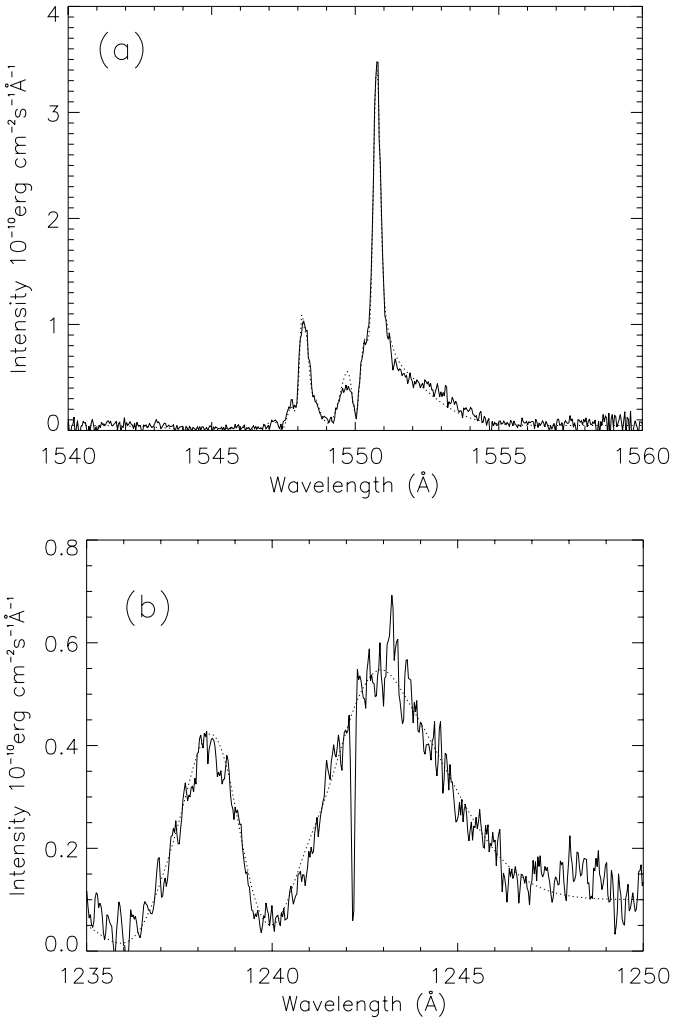

Fig. 7. The observed spectrum of AG Peg (solid) is compared to the fitted theoretical spectrum (dotted) for the resonance region of C IV (Fig. 7a) and N V (Fig. 7b). The observed spectra were recorded on 9 October 1979 (C IV) and 18 August 1978 (N V).

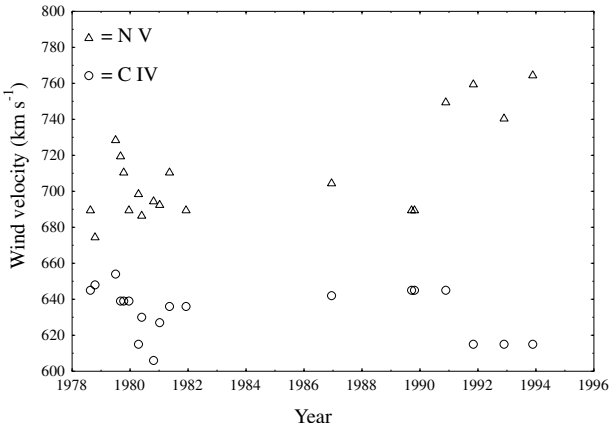

Fig. 8. Temporal behaviour of the white dwarf wind velocities of C IV and N V.

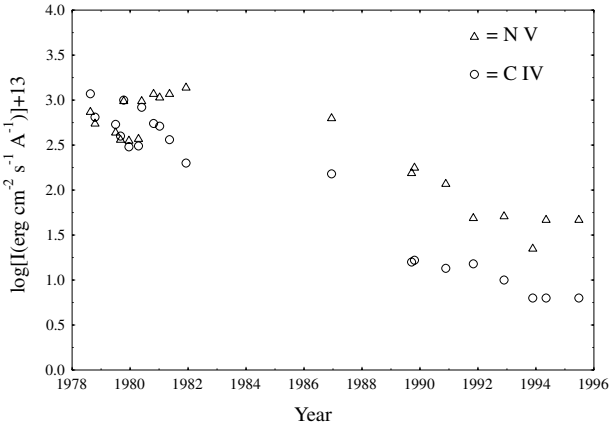

Fig. 9. C IV and N V peak intensities in the white dwarf wind. The last three circles (1994−1995) are to be treated as upper limits. Since the *FWHM* of the wind profiles was almost constant through the period (~2.5 Å for N V and ~2.1 Å for C IV) the total line fluxes follow the trends of the peak intensities. The sharp absorption at 1242.05 Å is a data artefact.

nearly a factor of three to $(2.6 \pm 1.1) \times 10^{-11}$ i.u., and the optical depth by almost a factor of five to 0.34 ± 0.08. After 1981, both the emission and the optical depth in the WD wind continue to decline. For the years 1994−1995 the intensity drops considerably and only upper limits can be derived. The optical depth and intensity of the N V lines obtained from the *IUE* observations Aug. 1978−Dec. 1981 are at levels of $\tau = 3.22 \pm 0.41$ and $I = (7.6 \pm 3.3) \times 10^{-11}$ i.u., respectively. During the ensuing 14 years, until the last *IUE* observation, the broad wind emission continually declines by about the same factor as C IV to $(2.3 \pm 1.1) \times 10^{-12}$ i.u., and the optical depth drops to 0.25 ± 0.04.

Two possibilities for the rapid decline of the broad wind component can be addressed: a decline in the density of the WD wind or an increase in the temperature of the white dwarf as it evolves to the left in the H-R diagram, ionizing C IV to C V and N V to N VI. Altamore & Cassatella (1997) analyzed the total flux in the He II Balmer α line relative to the continuum level at 1335 Å in AG Peg. Using the Zanstra method they found that the WD temperature was roughly constant for the period 1978−1995. Interestingly, the flux and opacity of the C IV lines decreased a few years earlier than the intensity and opacity of the N V lines (Figs. 9 and 10), which is expected if the temperature had increased during the 1980s.

The conditions for double scattering (Yoo et al. 2002) are fulfilled for C IV (the WD wind velocity larger than the fine structure separation), but not for N V. However, to get an effect on the blue line from the blue-shifted red line there is a need for an accelerating wind having two specific regions, where the velocity difference between the C IV ions matches the fine structure separation. This contradicts the nearly constant C IV velocity in the WD wind reported above and by Altamore & Cassatella (1997), and we find no arguments for including double scattering in our model.

5.2. The wind collision region

The strength of the C IV emission originating from the WC region drops by more than a factor of ten between December 1986 and September 1989 (Fig. 11). In the early observations the line intensity of the WC component of the red line varied

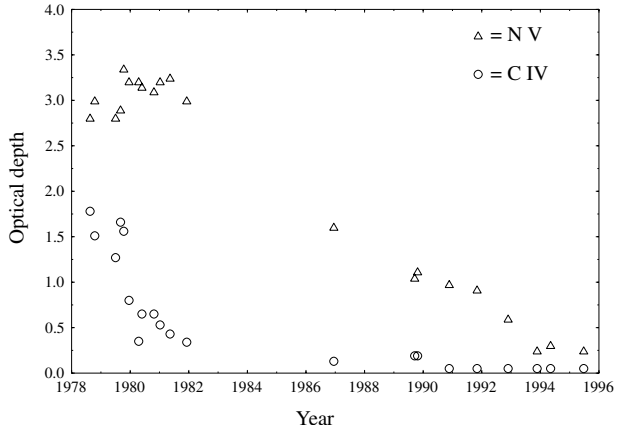

Fig. 10. C IV and N V line opacities in the white-dwarf wind in AG Peg.

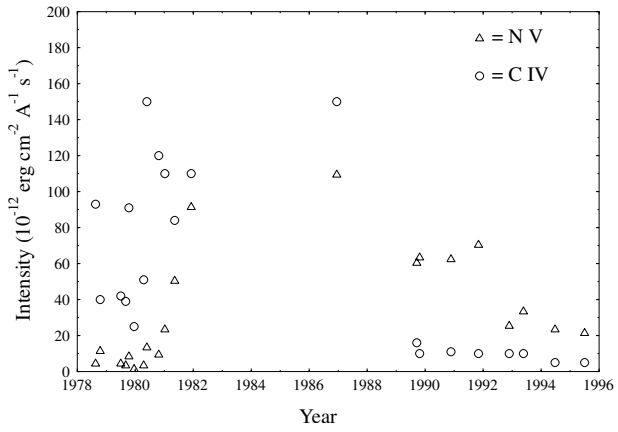

Fig. 11. Intensities in the wind-collision region in AG Peg.

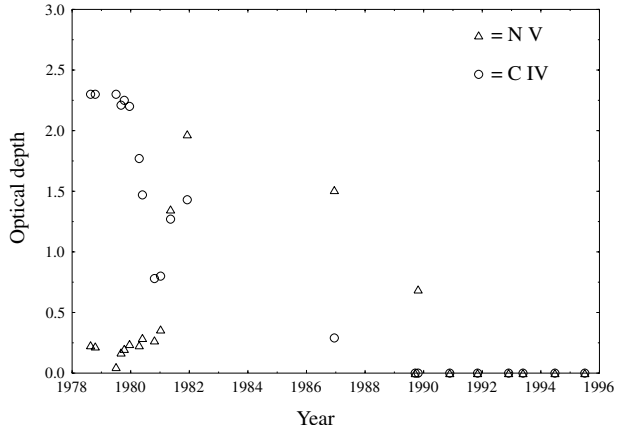

Fig. 12. Opacities in the wind-collision region in AG Peg.

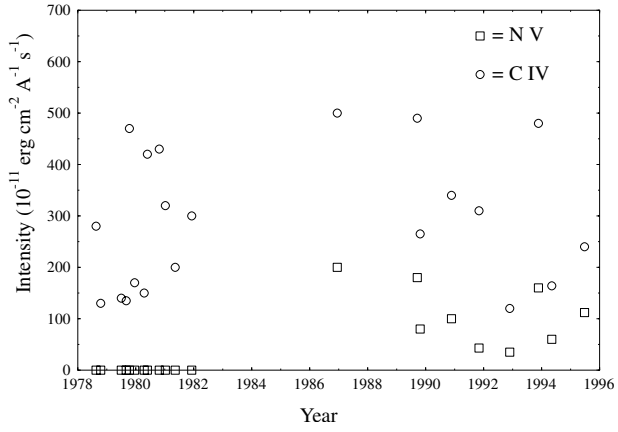

Fig. 13. Emission intensities from ionized part of red-giant wind in AG Peg.

in the interval $(0.3-1.5) \times 10^{-10}$ i.u., but later it decreased to $(1.1 \pm 0.3) \times 10^{-11}$ i.u. From August 1978 to December 1979 the optical depth for the blue-shifted absorption of the C IV doublet was 2.3 ± 0.2, but the lines are steadily vanishing and by 1989 there is no trace of absorption in the WC region (Fig. 12). The velocity shift of the blue-shifted absorption was 342 ± 24 km s^{-1} in late 1978, but it declined slowly and in December 1986 it was 280 ± 24 km s^{-1}. The velocity in the WC region is thus about half the WD velocity, which is expected according to the assumptions made in the introduction of Sect. 5. The lack of absorption in the spectra after 1986 makes it impossible to derive any velocity structure of the WC region from the fitting procedure. The disappearance of the blue-shifted absorption, while there is still emission in C IV, suggests that the decline of the WD wind emission is not only caused by an increase of its radiative temperature but also a decreased density. The temperature in the WC region is most likely due to mechanical heating and independent of the radiative temperature close to the white dwarf.

Until April 1980 the strength of the intensity of the N V emission from the WC region was $(5.5 \pm 2.8) \times 10^{-12}$ i.u., but then it increased and during 1980-1995 it has a mean value of $(4.5 \pm 2.1) \times 10^{-11}$ i.u. During the period 1978−1986 the optical depth in N V varied between 0.17 and 1.51 but the lines are absent in spectra recorded later than 1986. The velocity shift of the blue-shifted N V absorption in the WC region is 363 ± 33 km s^{-1} during 1978−1986.

5.3. The ionized part of the extended atmosphere of the red giant

The modeling of the C IV doublet reveals a double velocity structure of the red giant extended atmosphere, due to a fast wind at 144 ± 6 km s^{-1} and a slow wind at 59 ± 4 km s^{-1}. The slow wind is close to the expansion velocity of the inner nebular shell at 60 ± 15 km s^{-1} (Kenny et al. 1991). Both velocities stay constant through the entire period of *IUE* observations. During 1978 to 1981 and 1986 the optical depth in the fast wind is relatively high, $\tau = 1.69 \pm 0.09$, whereas it varies for the slow wind between 0.16 and 0.98 (Fig. 14). During 1989−1995 it appears stable around 0.75 ± 0.13 in the slow wind, but the opacity of the fast wind drops to 0.05 in 1989 and then is increasing to 0.67 during the last years of *IUE*. The intensity of the red C IV line is constant at $(3.1 \pm 1.9) \times 10^{-10}$ i.u. during the period (1978−1995).

There is no sign of a slow wind in the N V lines, whereas the fast wind is observable and has a velocity of 195 ± 19 km s^{-1}. It was not possible to derive an optical depth for N V in the first six SWP-spectra of AG Peg (Aug. 1978−Sep. 1979), but it increases steeply until December 1981 when it reached

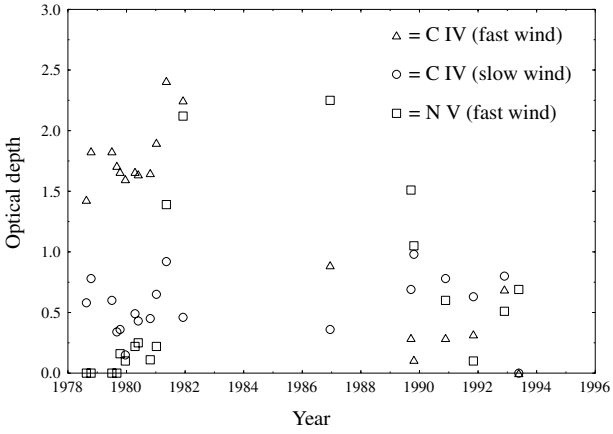

Fig. 14. Line opacities in ionized part of red-giant wind in AG Peg.

a value of 2.08 ± 0.48. It was also large in 1986 but after October 1989 it varied between 0.10 and 1.51. There is no N V resonance doublet emission from the RG atmosphere during 1978−1981. In December 1986 the narrow emission lines are observable and stay at a strength of $(1.26 \pm 0.66) \times 10^{-10}$ i.u. to the last *IUE* observations. This behaviour could be explained by the same phenomenon as the decline of the emission from the WD wind. When the radiation temperature in the WD wind becomes high enough to ionize N V more high energy photons will reach the extended RG atmosphere. This will lead to an increase in the temperature in the RG atmosphere and N IV will be ionized to N V.

5.4. The Fe II pumping channels

Fluorescence by the PAR mechanism turned out to be an important process to include when modeling the C IV doublet (Fig. 15). Since some Fe II fluorescence lines are excited by the narrow components of the C IV and N V lines the velocity (wavelength) shift between these and the pumped Fe II transitions is a good indicator of the velocity of the Fe II region. The best fit of the line profiles gives a velocity shift of ∼−15 km s^{-1} for N V and ∼+5 km s^{-1} for C IV. The line depth corresponding to the Fe II absorption is very different from one spectrum to another. This variation can be explained if the surrounding nebula is considered not to be homogeneous but split up into rather segmented regions of different density. However, the mean value of the pumping power for the $a^4F_{9/2}$−$y^4H_{11/2}$ and $a^4P_{1/2}$−$w^2D_{3/2}$ channels are 5.5×10^{-12} and 1.6×10^{-12} erg cm^{-2} s^{-1}, respectively. It is obtained as the deficit of the integrated intensity of the C IV doublet when the Fe II channel is incorporated To calculate the peak intensity, I_f of the fluorescence lines as a consequence of the pumping obtained from the observations we apply the formula:

$$I_f = \frac{E_p \cdot BF_f \cdot \lambda_p}{w_f \cdot \lambda_f}, \quad (7)$$

where BF_f is the branching fraction, λ_f wavelength and w_f the width of the fluorescence line. The parameters E_p and λ_p give the pumping power and the wavelength in the pumped channel, respectively. By using Eq. (5) an average peak intensity of Fe II λ2493.10 and λ2479.98 is calculated to be 3.5×10^{-12}

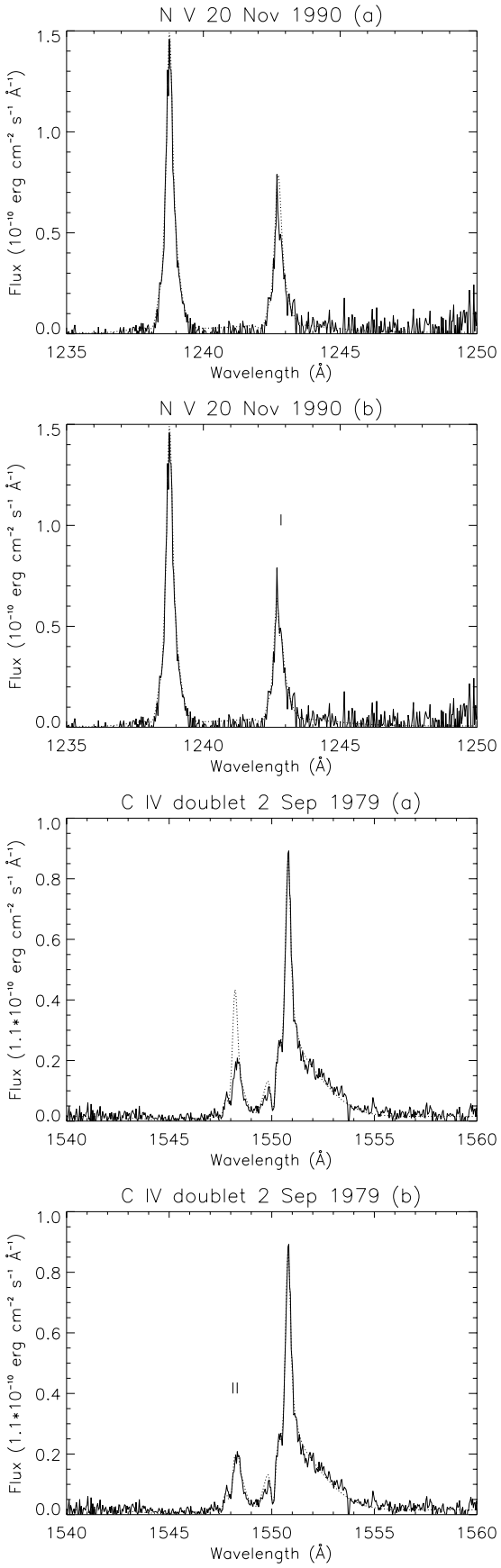

Fig. 15. Comparison between observed spectra of AG Peg (solid) and fits (dotted) of the C IV and N V doublets where the Fe II pumping channels (vertical lines) are not included **a)** or included **b)**.

and 3.1×10^{-12} erg cm^{-2} s^{-1} Å^{-1}, respectively. This is consistent with the line intensities given in Table 3, which correspond to the mean peak intensity as measured in LWP spectra, (4.4×10^{-12} and 3.3×10^{-12} erg cm^{-2} s^{-1} Å^{-1}, respectively). This agreement between the measured and calculated peak intensity of the Fe II fluorescence may serve as an indication of the validity of the fitted equation.

6. Conclusions

Spectra of AG Peg are very complicated but from this as well as previous work some general properties and evolutionary behaviour of the system are now revealed. A hot white dwarf ($T \sim 10^5$ K) and a red giant are orbiting each other with a period of slightly more than two years (Fekel et al. 2000). The two stars are embedded in a common envelope with an electron density higher than 10^{10} cm^{-3}. The wind collision region is mechanically heated to a level where highly-ionized elements emit spectral lines. On the part of the red giant facing the white dwarf the extended atmosphere is heated and ionized by the UV radiation from the white dwarf. Thus, the UV line spectrum of AG Peg has contributions from four different regions: the white dwarf wind, the ionized part of the red giant atmosphere, the wind collision region and the common envelope.

The C IV and N V resonance doublets have very complex line profiles, which contain useful information about all four regions simultaneously. Three of the regions (the WD wind, ionized part of the RG atmosphere and the WC region) give contibutions to the emission lines as well as to the absorption, whereas Fe II in the fourth region (the common envelope) is pumped by these lines and therefore affects their profiles. By modeling the N V and C IV resonance doublets we obtained values of the optical depths, expansion velocites, intensities and information about the development of these parameters during the time of *IUE* observations.

Both intensity and opacities have decreased in the white dwarf wind, which we believe is due to a temperature increase since the intensity of the C IV doublet started to decline at least two years before the N V doublet. Emission of the N V doublet in the ionized part of the red giant was not observed until 1986 when the opacity in the white dwarf wind had started to decrease. This is consistent with an increase of the temperature in the white dwarf wind that would lead to more UV photons reaching the atmosphere of the red giant. The modeling of C IV showed two different expansion velocities for the red giant atmosphere (144 and 59 km s^{-1}) while only the higher expansion velocity was obtained when modeling N V.

Acknowledgements. All of the data presented in this paper were obtained from the Multimission Archive at the Space Telescope Science Institute (MAST). STScI is operated by the Association of Universities for Research in Astronomy, Inc., under NASA contract NAS5-26555. Support for MAST for non-HST data is provided by the NASA Office of Space Science via grant NAG5-7584 and by other grants and contracts. We are grateful to the referee, A. Cassatella, for detailed examination of the manuscript and for valuable criticism and suggestions for its improvements.

Appendix A: The equation fitted to C IV doublet

The results of modeling the C IV and N V resonance doublets have been described in Sect. 5. Here we present the input parameters and equations used to provide the model line profile. The final equations F^X (X = C(arbon) or N(itrogen)) account for radiative origins from the different regions in the symbiotic system. For each region we define parameters for intensity of radiation I, expansion velocity v, optical depth τ, and line width w. We start by computing the emitted energy in each component of the doublet, assuming that the longer-wavelength component has a certain intensity and the shorter wavelength component is twice this value.

I_i^X = Intensity of the red component.
v_i^X = Expansion velocity.
τ_i^X = Optical depth for the red component.
w_i^X = Gaussian width.
u_i^X = Velocity of region i relative to the Fe II region.
$\lambda_{\rm b}^X$ = Lab wavelength of the blue line.
$\lambda_{\rm r}^X$ = Lab wavelength of the red line.
$\tau_j^{\rm Fe}$ = Optical depth for Fe II.
λ_j = Wavelength for Fe II channel.
$w_{\rm Fe}$ = Gaussian width of Fe II absorption.
$v_{\rm Fe}$ = Expansion velocity of surrounding Fe II region.
c = Speed of light.
h^X = Continuum level.

The index i stands for:

1 = white dwarf wind;
2 = slow component in red giant wind;
3 = fast component in red giant wind;
4 = collision region;
5 = continuum source.

The index j stands for:

1 = Fe II line at 1548.204 Å;
2 = Fe II line at 1548.411 Å;
3 = Fe II line at 1548.697 Å;
4 = Fe II line at 1242.741 Å.

The equations

The d_i^X functions describe the energy emitted by the C IV and N V resonance doublets. Wavelength dependence has been surpressed in the equations.

$$d_i^X = I_i^X \cdot \mathrm{e}^{-\frac{\left(\lambda+\lambda_{\rm r}^X\cdot\left(u_i^X c^{-1}-1\right)\right)^2}{\left(w_i^X\right)^2}} + 2\cdot I_i^X \cdot \mathrm{e}^{-\frac{\left(\lambda+\lambda_{\rm b}^X\cdot\left(u_i^X c^{-1}-1\right)\right)^2}{\left(w_i^X\right)^2}} \quad (0 < i < 5)$$

$$d_5^X = h^X.$$

The k_i^X functions ($0 < i < 6$) describe the fraction of the emission that passes through each of the regions into our line of sight.

O_{it}^X = Fraction of light from region i that passes through region t

$$k_i^X = \sum_{t=1}^{5} d_t^X O_{it}^X.$$

The functions a_i^X $(0 < i < 5)$ describe the absorption of the doublet in the discussed regions.

$$a_i^X = \left(\mathrm{e}^{-\tau_i^X} - 1\right) \cdot \mathrm{e}^{-\frac{\left(\lambda + \lambda_t^X \cdot \left(\left(u_i^X + v_t^X\right) c^{-1} - 1\right)\right)^2}{\left(w_i^X\right)^2}} \cdot k_i^X + \left(\mathrm{e}^{-2\tau_i^X} - 1\right) \cdot \mathrm{e}^{-\frac{\left(\lambda + \lambda_b^X \cdot \left(\left(u_i^X + v_t^X\right) c^{-1} - 1\right)\right)^2}{\left(w_i^X\right)^2}} \cdot k_i^X.$$

The function A^X describes the profile of the doublet before it reaches the Fe^+ ions.

$$A^X = \sum_{i=1}^{5} d_i^X + \sum_{i=1}^{4} a_i^X,$$

while the functions f_j^X describe the absorption by Fe^+ ions.

$$f_j^X = \left(\mathrm{e}^{-\tau_j^{\mathrm{Fe}}} - 1\right) \cdot \mathrm{e}^{-\frac{\left(\lambda + \lambda_j \cdot \left(v_{\mathrm{Fe}} c^{-1} - 1\right)\right)^2}{\left(w_{\mathrm{Fe}}\right)^2}} \cdot A^X.$$

F^X is the final result that describes the theoretical profile of the doublet which has been compared to the observed spectra.

$$F^X = A^X + \sum_j f_j^X.$$

References

Allen, D. A. 1980, MNRAS, 190, 75
Allen, D. A. 1982, Nature of Symbiotic Stars, ed. M. Friedjung, & R. Viotti (Reidel: Dordrecht), IAU Coll., 70, 27
Allen, D. A. 1983, MNRAS, 204, 1009
Altamore, A., & Cassatella, A. 1997, A&A, 317, 712
Boffi, F. R., Branch, D., & Baron, E. 1994, A&AS, 184, 5707
Chakrabarty, D., van Kerwijk, M. H., & Larkin, J. E. 1998, ApJ, 497, 39
Eriksson, M., Johansson, S., & Wahlgren, G. M. 2001, ed. T. R. Gull, S. Johansson, & K. Davidsson (San Francisco: ASP), ASP Conf. Ser., 242, 325
Fekel, F. C., Joyce, R. R., Hinkle, K. H., & Skrutskie, M. F. 2000, AJ, 119, 1375
Fuhr, J. R., Martin, G. A., & Wiese, W. L. 1988, J. Phys. Chem. Ref. Data Suppl., 17, 4
Gallagher, J. S., Holm, A. V., Andersson, C. M., & Webbink, R. F. 1979, ApJ, 229, 994
Girard, T., & Willson, L. A. 1987, A&A, 183, 247
Johansson, S. 1983, MNRAS, 205, 71
Hartman, H., & Johansson, S. 2000, A&A, 359, 627
Kenyon, S. J., Mikolajewska, J., & Mikolajewski, M. 1993, AJ, 106, 1573
Kenyon, S. J., & Webbink, R. F. 1984, ApJ, 279, 252
Kenny, H. T., Taylor, A. R., & Seaquist, E. R. 1991, ApJ, 366, 549
Keyes, C. E., & Plavec, M. J. 1980, NASA-GSFC Symp., The Universe in Ultraviolet Wavelengths, ed. R. Chapman (NASA CP-2717), 443
Lundmark, K. 1921, AN, 213, 93
Meier, S. R., Kafatos, M., & Fahey, R. P. 1994, ApJS, 94, 183
Merril, P. W. 1951, ApJ, 113, 605
Michalitsianos, A. G., Kafatos, M., & Meier, S. R. 1992, ApJ, 389, 649
Munari, U. 1994, MmSAI, 65, 157
Mürset, U., Jordan, S., & Walder, R. 1995, A&A, 297, 87
Mürset, U., Wolff, B., & Jordan, S. 1997, A&A, 317, 712
Nussbaumer, H. 1982, Nature of Symbiotic Stars, ed. M. Friedjung, & R. Viotti (Dordrecht: Reidel), IAU Colloq., 70, 85
Nussbaumer, H., Schmutz, W., & Vogel, M. 1995, A&A, 293, L13
Penston, M. V., & Allen, D. A. 1985, MNRAS, 212, 939
Phillips, J. P. 1998, A&A, 340, 527
Tomov, N., & Tamova, M. 2001, Ap&SS, 278, 311
Vogel, M., & Nussbaumer, H. 1994, A&A, 248, 145
Warner, B. 1968, MNRAS, 141, 273
Yoo, J. J., Lee, H., & Ahn, S. 2002, MNRAS, 334, 974